INSTITUTE FOR NUCLEAR STUDY
UNIVERSITY OF TOKYO
Tanashi, Tokyo 188
Japan

INS-Rep.-575
March 1986

Yet Another Monte Carlo Study of the Schwinger Model*)

K. Sogo and N. Kimura

INS-Rep.-575
March 1986

Yet Another Monte Carlo Study of the Schwinger Model*)

K. Sogo and N. Kimura

Institute for Nuclear Study,
University of Tokyo,
Tanashi, Tokyo, 188, Japan

Abstract

Some methodological improvements are introduced in the quantum Monte Carlo simulation of the 1+1 dimensional quantum electrodynamics (the Schwinger model). Properties at finite temperatures are investigated, concentrating on the existence of the chirality transition and of the deconfinement transition.

---

*) Talk given by K. S. at the 1985 INS Winter Seminar, held on Dec. 16-18, 1985.

§1. Introduction

The Schwinger model (we imply by this both massless and massive case) is quantum electrodynamics (QED) of Dirac particles of mass m and charge g in 1+1 dimensional space-time. The Lagrangian is given by

$$L = -\frac{1}{4} F_{\mu\nu}F^{\mu\nu} + \bar{\psi}(i\not{\partial}-m)\psi \ , \qquad (1)$$

where

$$F_{\mu\nu} = \partial_\mu A_\nu - \partial_\nu A_\mu$$

$$\not{\partial} = \gamma^\mu(\partial_\mu + igA_\mu) \ .$$

Since the pioneering paper by Schwinger,[1] many aspects of the model have been investigated almost thoroughly.[2),3] Especially the massless Schwinger model has attracted much attention, because it possesses two significant properties such as the confinement and the chiral symmetry breaking in the ground state. And such properties are expected also for quantum chromodynamics (QCD) in 3+1 dimensional space-time. Knowledge about the dynamics of the Schwinger model would give us, therefore, some imaginations to the dynamics of QCD. From this viewpoint, it is a very appealing question to ask whether the Schwinger model experiences a deconfinement transition and/or a chirality restoring transition at finite temperature. It is one of our motivations to clarify this problem by Monte Carlo (MC) simulation.

The Schwinger model formulated on the lattice have also served as a testing field of various methods and techniques in the MC simulations of lattice gauge theories. There have appeared by now many works[4)~6)] on MC simulations of the lattice Schwinger model. These works can be classified into three groups:

a) pseudo fermion method or quenched approximation,[4)]

b) local Hamiltonian method,[5)]

c) Langevin equation method,[6)]

where the references are certainly not exhaustive. Among these procedures the second one is, in our opinions, the most trustworthy approach. The applicability of the method is, however, limited to 1+1 dimension due to the notorious "negative sign problem" in higher dimensions. And in this sense the third method is the most promissing approach because it treats both fermion fields and gauge fields at the same time, and it works in arbitrary dimensions.

In this note we apply the local Hamiltonian method to the lattice Schwinger model. Some improvements, details of which are described in §2, are introduced in the MC method, which is another one of the motivations of this note. The organization of the paper is as follows. In the next section §2, we describe the method of the MC simulation for the lattice Schwinger model. The results of the simulation are shown in §3. The last section §4 is summary and discussions. Some technical details are included in accordance with the purport of the Proceedings of the INS Winter Seminar.

§2. Method of the Monte Carlo Simulation

(1) Lattice Hamiltonian

In order to use the local Hamiltonian method, we formulate the model on a lattice according to Kogut and Susskind.[7] By choosing the gauge $A_0 = 0$, the resulting lattice Hamiltonian is given by[5]

$$H = \sum_{n=1}^{N} H_{n,n+1} ,$$

$$H_{n,n+1} = \frac{g^2}{2} \cdot a \cdot L_n^2 - \frac{i}{2a} \cdot (\psi_n^+ a_n^+ \psi_{n+1} - \psi_{n+1}^+ a_n \psi_n) + \frac{m}{2} \cdot (-1)^n (\psi_n^+ \psi_n - \psi_{n+1}^+ \psi_{n+1}) , \tag{2}$$

where a is the lattice spacing; operators L_n, a_n^+ and a_n obey the commutation relations,

$$[L_m, a_n^+] = + a_n^+ \delta_{mn} ,$$
$$[L_m, a_n] = - a_n \delta_{mn} . \tag{3}$$

The operator a_n comes from $\exp(iga \cdot A_1(n))$, and the operator L_n stands for the conjugate momentum to $A_1(n)$, that is, $gL_n = \pi_{A_1(n)}$. Now let us make further transformation from the (ψ_n, ψ_n^+) representation to the (χ_n, χ_n^+) representation,

$$\psi_n = (-i)^n \chi_n , \qquad \psi_n^+ = (+i)^n \chi_n^+ , \tag{4}$$

which changes Hamiltonian (2) into the new Hamiltonian,

$$H_{n,n+1} = \frac{g^2}{2} \cdot a \cdot L_n^2 - \frac{1}{2a} \cdot (\chi_n^+ a_n^+ \chi_{n+1} + \chi_{n+1}^+ a_n \chi_n)$$

$$+ \frac{m}{2} \cdot (-1)^n (\chi_n^+ \chi_n - \chi_{n+1}^+ \chi_{n+1}) \quad . \tag{5}$$

The Hamiltonian (5) describes a coupled system of scalar fermions and gauge bosons. The operators χ_n and χ_n^+ obey the anticommutation relations,

$$\{\chi_m, \chi_n^+\} = \delta_{mn} \quad ,$$

$$\{\chi_m, \chi_n\} = \{\chi_m^+, \chi_n^+\} = 0 \quad . \tag{6}$$

(2) Local Hamiltonian method

We consider canonical ensemble of the system, which is described by the partition function,

$$Z = \mathrm{Tr}\, e^{-\beta H} \quad , \tag{7}$$

In the local Hamiltonian method[8] we first apply Trotter's formula to eq. (7); we cut the β-direction into L slices and then divide each into two parts,

$$Z = \mathrm{Tr}(e^{-(\beta/L)H})^L \simeq \mathrm{Tr}(U_1 U_2)^L \tag{8}$$

where we put $H = H_1 + H_2$,

$$U_{1(2)} = \exp(-\Delta\tau \cdot H_{1(2)}) \ ,$$

$$H_{1(2)} = \sum_{n=\text{odd(even)}} H_{n,n+1} \ , \tag{9}$$

with $\Delta\tau = \beta/L$. After this decomposition the operator $U_{1(2)}$ is factorized into a product of operators because terms in $H_{1(2)}$ commute with each other. The approximation (8) is justified as far as $\Delta\tau$ is sufficiently small. Practically it is known that values $\Delta\tau = 0.1 \sim 0.3$ are good enough in many examples[8),9)]; we fix the value $\Delta\tau = 0.2$ in this note. Temperature T of the system is, therefore, controlled by the value of L, according to the formula $T = (\Delta\tau \cdot L)^{-1}$.

In this way we formulate the problem of computing the partition function as a stochastic process of the fermion and boson states on a checkerboard. And this process is simulated by importance sampling of MC method (heat bath algorithm).

In order to implement this procedure in computers, we need matrix elements of the operator $U = \exp(-\Delta\tau \cdot H_{n,n+1})$. For this purpose we decompose $H_{n,n+1}$ into

$$H_{n,n+1} = H_G + H_{FG} \ , \tag{10}$$

where

$$H_G = \frac{g^2}{2} \cdot a \cdot L_n^2 \ ,$$

$$H_{FG} = -\frac{1}{2a}(\chi_n^+ a_n^+ \chi_{n+1} + \chi_{n+1}^+ a_n \chi_n) + \frac{m}{2}(-1)^n (\chi_n^+ \chi_n - \chi_{n+1}^+ \chi_{n+1}) . \tag{11}$$

According to the Baker-Campbell-Hausdorff formula we have

$$U = \exp\left[-\Delta\tau(H_G + H_{FG})\right]$$

$$= e^{-\frac{\Delta\tau}{2}H_G} e^{-\Delta\tau H_{FG}} e^{-\frac{\Delta\tau}{2}H_G} e^{R} , \qquad (12)$$

where the remaining term R is

$$R = \frac{1}{12}\cdot(\Delta\tau)^3\left[\left[H_G, H_{FG}\right], H_{FG}\right] + 0(\Delta\tau)^4 , \qquad (13)$$

which is of the third order in $\Delta\tau$. We can use

$$U_0 = e^{-\frac{\Delta\tau}{2}H_G} e^{-\Delta\tau H_{FG}} e^{-\frac{\Delta\tau}{2}H_G} , \qquad (14)$$

instead of U. Now it is easy to calculate the matrix elements of U_0, and we show them in Table 1. In the table we introduced

$$A = \frac{e^{(\Delta\tau/2a)ch\theta}}{1 + e^{-2\theta}} + \frac{e^{-(\Delta\tau/2a)ch\theta}}{1 + e^{2\theta}} ,$$

$$B = \frac{e^{(\Delta\tau/2a)ch\theta}}{1 + e^{2\theta}} + \frac{e^{-(\Delta\tau/2a)ch\theta}}{1 + e^{-2\theta}} ,$$

$$C = \frac{e^{(\Delta\tau/2a)ch\theta} - e^{-(\Delta\tau/2a)ch\theta}}{e^{\theta} + e^{-\theta}} , \qquad (15)$$

where θ is defined by $sh\theta = 2ma$.

Table 1

It should be noted here that the matrix elements in Table 1 are different from those of Schiller and Ranft,[5] who decomposed H_{FG} further into the kinetic term H_K and the mass term H_M. That is, they used

$$U_{SL} = e^{-\frac{\Delta\tau}{2}H_M} e^{-\frac{\Delta\tau}{2}H_G} e^{-\Delta\tau H_K} e^{-\frac{\Delta\tau}{2}H_G} e^{-\frac{\Delta\tau}{2}H_M} , \quad (16)$$

instead of U_0 for the approximation to the operator U. The error in U_0 to the true U is estimated, as is shown before, to be of the order

$$(\Delta\tau)^3 \cdot g^2 a \cdot (\max(m, a^{-1}))^2 . \quad (17)$$

On the order hand, the error in U_{SL} is of the order

$$(\Delta\tau)^3 \cdot \{ g^2 a \cdot (\max(m, a^{-1}))^2 + m^2 a^{-1} + m \cdot a^{-2} \} , \quad (18)$$

which contains two more factors independent of the gauge coupling g. For the case of large m and/or small g, this difference would cause deviations from the real physical processes in the simulations.

Let us comment here on dimensions and scales of relevant quantities. Because we are using the natural unit, all the quantities are scaled by only one parameter $a^{-1} \equiv \Lambda$, which is a cut-off with mass dimension. And all other parameters are

measured physically by dimensionless combinations with a, such as the gauge coupling by ga, the fermion mass by ma, and the temperature by $Ta = a/(\Delta\tau \cdot L)$. In this note we fix a=1, and vary these dimensionless parameters within the region [0,1].

(3) Symmetric measurement

Finally let us explain the way of measurements. The procedure employed here is the one suggested recently by Suzuki,[10] which have some advantages over previous ones.[5),8),9)] The point of this method is as follows. Previously the average of an operator A was computed in MC simulations by the formula[8)]

$$\langle A \rangle = Z^{-1} \cdot \mathrm{Tr}(Ae^{-\beta H})$$

$$= \sum_{\{i\}} \left\{ \frac{\langle i_i | A_1 U_1 | i_2 \rangle}{\langle i_1 | U_1 | i_2 \rangle} + \frac{\langle i_{2L} | U_2 A_2 | i_1 \rangle}{\langle i_{2L} | U_2 | i_1 \rangle} \right\} P(i_1, \cdots, i_{2L}) \quad , \quad (19)$$

$$P(i_1, \cdots, i_{2L}) = \langle i_1 | U_1 | i_2 \rangle \langle i_2 | U_2 | i_3 \rangle \cdots \langle i_{2L} | U_2 | i_1 \rangle \quad ,$$

where we assumed A is decomposed into $A = A_1 + A_2$ as Hamiltonian is. Now in the symmetric measurement the same quantity is computed by the formula

$$\langle A \rangle = \sum_{\{i\}} \left\{ \frac{\langle i_1 | U_1^{1/2} A_1 U_1^{1/2} | i_2 \rangle}{\langle i_1 | U_1 | i_2 \rangle} + \frac{\langle i_{2L} | U_2^{1/2} A_2 U_2^{1/2} | i_1 \rangle}{\langle i_{2L} | U_2 | i_1 \rangle} \right\} P(i_1, \cdots, i_{2L}), \quad (20)$$

which implements the inversion symmetry with respect to β-direction. In other words, stationarity of the equilibrium is regarded automatically in eq. (20), which ensures the accuracy of measurements.

In such a symmetrized way are measured the quantities:

a) internal energy, $\langle H \rangle$,

b) charge and current, $\langle j_0 \rangle$ and $\langle j_1 \rangle$,

c) chirality, $\langle \bar{\psi}\psi \rangle$,

d) charge correlations, $F_k(\tau) = \langle j_0(k,\tau) j_0(-k,0) \rangle$.

On the discrete lattice these operators are expressed by[7]

$$j_0 = \bar{\psi}\gamma_0\psi \to a^{-1} \cdot (\chi_n^+\chi_n + \chi_{n+1}^+\chi_{n+1}) \ ,$$

$$j_1 = \bar{\psi}\gamma_1\psi \to a^{-1} \cdot (-i)(\chi_n^+\chi_{n+1} - \chi_{n+1}^+\chi_n) \ ,$$

$$\bar{\psi}\psi \to a^{-1} \cdot (-1)^n (\chi_n^+\chi_n - \chi_{n+1}^+\chi_{n+1}) \ ,$$

and

$$j_0(k,0) \longrightarrow \frac{1}{Na} \cdot \sum_{n=1}^{N} e^{ikn} \chi_n^+\chi_n$$

$$j_0(k,\tau) \longrightarrow (U_1U_2)^{-\tau} j_0(k,0) (U_1U_2)^{+\tau} \ . \qquad (21)$$

Results of MC measurements of these quantities for various values of parameters g, m and T are shown in the next section.

§3. Results of Simulations

Our results are obtained from the MC data of 10000 MC sweeps after 5000 sweeps of thermalization on the system with N = 40 and L = 5∿40.

a) Internal energy

In Fig.1 the internal energy is depicted against temperature for typical cases of massless and massive. The curves are monotonously increasing functions of the temperature without abrupt changes, which indicates non-existence of critical point in thermodynamic functions.

Fig. 1

b) Charge and current

Measured values of these quantities always vanish exactly, as is expected. Since both the total charge and the total current commute with Hamiltonian, these quantities remain at the same value of the initial state, i.e., the vacuum.

c) Chirality

First Let us see the massless case. In Fig. 2 the chiral order parameter $\langle\bar{\Psi}\psi\rangle$ is shown for the gauge coupling g. Because the chirality $\langle\bar{\Psi}\psi\rangle$ has a mass dimension, it will be expressed, in general, by

$$\langle\bar{\Psi}\psi\rangle = a^{-1}f(ga) \ , \tag{22}$$

in terms of the dimensionless quantity ga. Now from Fig.2 we know that the function f has limiting values $f(0) = 0$ and $f(\infty) = 1$. And the continuum limit is achieved by considering $ga \ll 1$; we have from eq. (22)

$$\langle \bar{\psi}\psi \rangle \simeq g \cdot f'(0), \qquad ga \ll 1 . \tag{23}$$

From Fig.2 the value f'(0) is estimated as

$$f'_{MC}(0) = 0.21 . \tag{24}$$

On the other hand the continuum theory gives

$$f'_{exact}(0) = \frac{e^{\gamma}}{2\pi^{3/2}} \simeq 0.16 , \tag{25}$$

which is close to the MC value (24). It should be remembered that from a purely theoretical point of view the behavior outside of the scaling region is merely an artifact on the discrete lattice and is not related to the original problem in the field theory.

Fig. 2 & Fig. 3

Next let us see the cases with non-zero mass. In Fig.3 the chirality $\langle \bar{\psi}\psi \rangle$ is plotted against the gauge coupling g for several values of mass m. Because the mass term breaks the chiral symmetry explicitly, the finite mass m dominates the behavior of $\langle \bar{\psi}\psi \rangle$, which can be seen clearly in Fig.3. However, if we apply the same argument as in the massless case, we immediately recognize that we should deal with the function $\langle \bar{\psi}\psi \rangle$ of the gauge coupling g, not for the fixed value m, but for the fixed ratio m/g, as is shown in Fig.4. The argument goes as follows.

The chirality $\langle\bar{\psi}\psi\rangle$ is expressed by

$$\langle\bar{\psi}\psi\rangle = a^{-1}\tilde{f}(ga,m/g) \ , \tag{26}$$

in terms of dimensionless quantities ga and m/g. In the continuum limit (or the scaling regime), we have from eq. (26)

$$\langle\bar{\psi}\psi\rangle \simeq g\cdot\tilde{f}'(0,m/g), \quad ga \ll 1, \quad \text{fixed } m/g \ , \tag{27}$$

where the coefficient $\tilde{f}'(0,m/g)$ is the partial derivative of function $\tilde{f}$ and depends only on the ratio m/g. Fig.4 shows the existence of such scaling region. The estimated values of the coefficient $\tilde{f}'(0,m/g)$ are given in Fig.5.

Fig. 4 & Fig. 5

Lastly let us see the temperature dependence of the chirality. In Fig.6 the chirality $\langle\bar{\psi}\psi\rangle$ is depicted against temperature for typical cases of massless and massive. The curves indicate non-existence of critical temperature for the chirality as well.

Fig. 6

d) Charge correlation

Finally we consider the (imaginary) time correlation

function of the charge fluctuation with momentum k: $F_k(\tau) = \langle j_0(k,\tau) j_0(-k,0) \rangle$. In Fig.7 is shown a typical shape of the function $F_k(\tau)$, from which we can extract a physical mass m_{ph} by fitting each curve with the formula

$$F_k(\tau) = F_0 \cdot (e^{-\tau \cdot E(k)} + e^{-(L-\tau) \cdot E(k)}) , \tag{28}$$

$$E(k) = \sqrt{(m_{ph}a)^2 + k^2} . \tag{29}$$

A detailed analysis on this issue will be given in a future publication.

Fig. 7

§4. Summary and Discussions

We have reexamined the Monte Carlo simulation of the 1+1 Schwinger model by introducing new methodological improvements, i.e., more precise matrix elements for the transfer matrix and the symmetric measurement method. More appropriate analysis than previous authors[5] is performed on the continuum limit and the scaling behavior. The results show that there is no finite critical temperature in the Schwinger model both in the chirality and in the confinement. In other words, we have found that $T_\chi = T_c = \infty$, which is consistent with the inequality $T_\chi \geq T_c$ by Casher.[11]

There are many problems left, which is related to the Schwinger model. First, generalization to the non-Abel group and/or the multi-flavor case is very appealing.[12] Second, it will be important to compare the Langevin equation method with the local Hamiltonian method on the same model, say, the Schwinger model. Finally it is very pleasing that a similar system as the Schwinger model exists in condensed matter physics as a model of polyacetylene,[13] although the Hamiltonian is not exactly the same.

Acknowledgements

The authors are very grateful to the members of theory division at INS. The numerical calculation was done by FACOM M-380 at the INS computer center.

References

1) J. Schwinger, Phys. Rev. 128 (1962) 2425.

2) J. Lowenstein and J. Swieca, Ann. of Phys. 68 (1971) 172;
S. Coleman, R. Jackiw and L. Susskind, ibid. 93 (1975) 267;
S. Coleman, ibid. 101 (1976) 239.

3) J. Kogut and L. Susskind, Phys. Rev. D11 (1975) 3594;
T. Banks and L. Susskind, ibid. D13 (1976) 1043;
W. Fischler, J. Kogut and L. Susskind, ibid. D19 (1979) 1188.

4) H.W. Hamber, Phys. Rev. D24 (1981) 951;
E. Marinari, G. Parisi and C. Rebbi, Nucl. Phys. B190 FS3 (1981) 734;
A. Duncan and M. Furman, ibid. B190 FS3 (1981) 767.

5) O. Martin and S. Otto, Nucl. Phys. B203 (1982) 297;
A. Schiller and J. Ranft, ibid. B225 FS9 (1983) 204.

6) H. Gausterer and J.R. Klauder, Phys. Rev. Lett. 56 (1986) 306.

7) J. Kogut and L. Susskind, Phys. Rev. D11 (1975) 395.
J. Kogut, Rev. Mod. Phys. 55 (1983) 775.

8) J.E. Hirsch, R.L. Sugar, D.J. Scalapino and R. Blankenbecler, Phys. Rev. B26 (1982) 5033.

9) R.T. Scaletter, D.J. Scalapino and R.L. Sugar, Phys. Rev. B31 (1985) 7316;
A. Nakamura, K. Sogo and M. Uchinami, Phys. Lett. 111A (1985) 71;
K. Sogo and M. Uchinami, to be published in J. Phys. A 1986.

10) M. Suzuki, to be published in J. Stat. Phys. 1986.

11) A. Casher, Phys. Lett. 83B (1979) 395.

12) M. Hellmund, Phys. Lett. 166B (1986) 214.

13) D.K. Campbell, T.A. DeGrand and S. Mazumdar, Phys. Rev. Lett. 52 (1984) 1717.

Figure captions

Fig. 1. The internal energy versus temperature.

Fig. 2. The chirality versus gauge coupling for the massless Schwinger model.

Fig. 3. The chirality versus gauge coupling for the massive Schiwnger model.

Fig. 4. The chirality versus gauge coupling with fixed m/g ratio.

Fig. 5. The estimated values of the coefficient $\tilde{f}'(0,m/g)$. The ✖ mark is the exact result 0.16.

Fig. 6. Temperature dependence of the chirality.

Fig. 7. The charge correlation function.

Table 1. Matrix elements of $U = \exp(-\Delta\mathcal{C}\cdot H_{n,n+1})$.

	$\exp(-\frac{1}{2}g^2 a\,\Delta\tau\cdot m^2)$
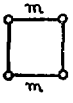	$\exp(-\frac{1}{2}g^2 a\,\Delta\tau\cdot m^2)$
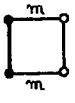	$\exp(-\frac{1}{2}g^2 a\,\Delta\tau\cdot m^2)\cdot\begin{cases} A & n = \text{odd} \\ B & n = \text{even} \end{cases}$
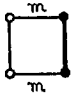	$\exp(-\frac{1}{2}g^2 a\,\Delta\tau\cdot m^2)\cdot\begin{cases} B & n = \text{odd} \\ A & n = \text{even} \end{cases}$
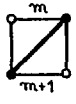	$\exp[-\frac{1}{4}g^2 a\,\Delta\tau\cdot\{m^2+(m+1)^2\}]\cdot C$
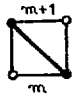	$\exp[-\frac{1}{4}g^2 a\,\Delta\tau\cdot\{m^2+(m+1)^2\}]\cdot C$

Table 1

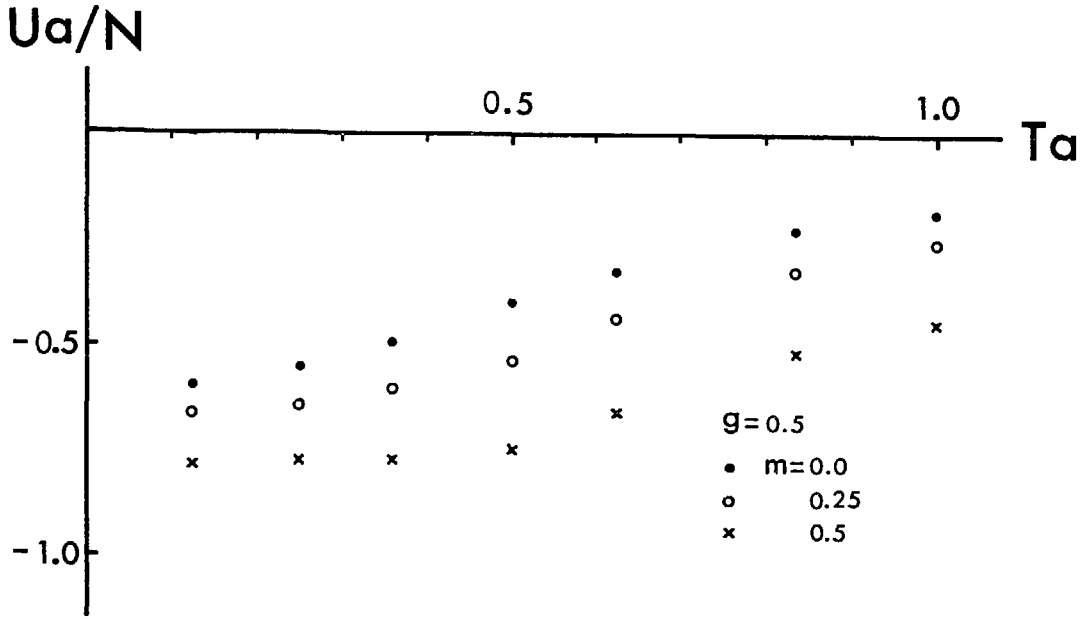

Fig.1

Fig.1

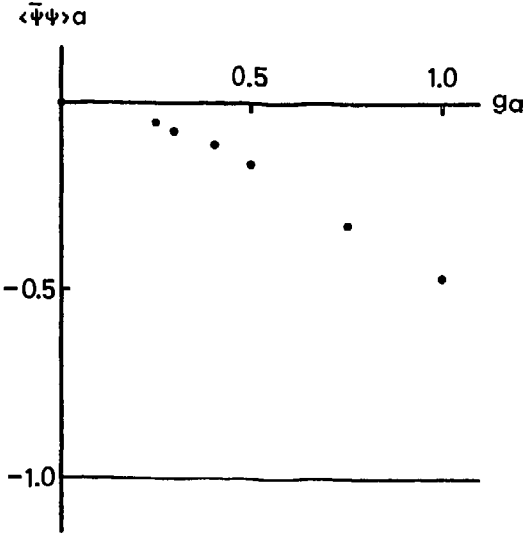

Fig. 2

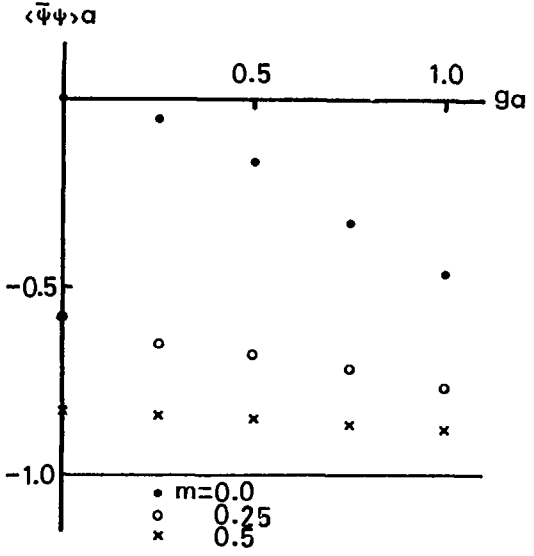

Fig. 3

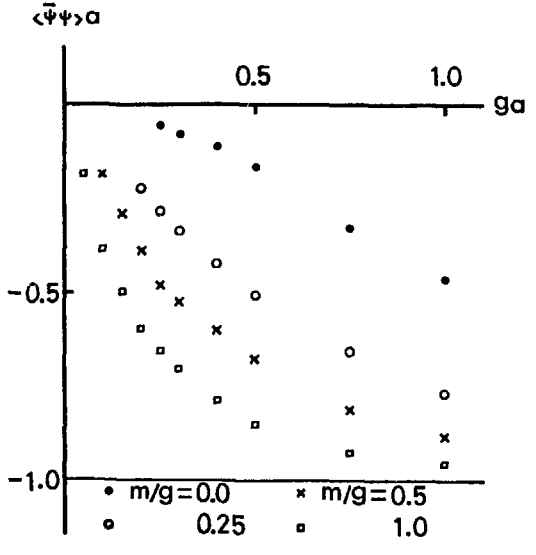

Fig. 4

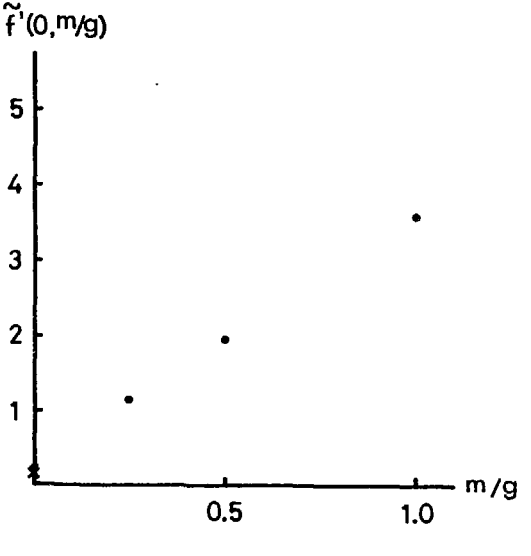

Fig. 5

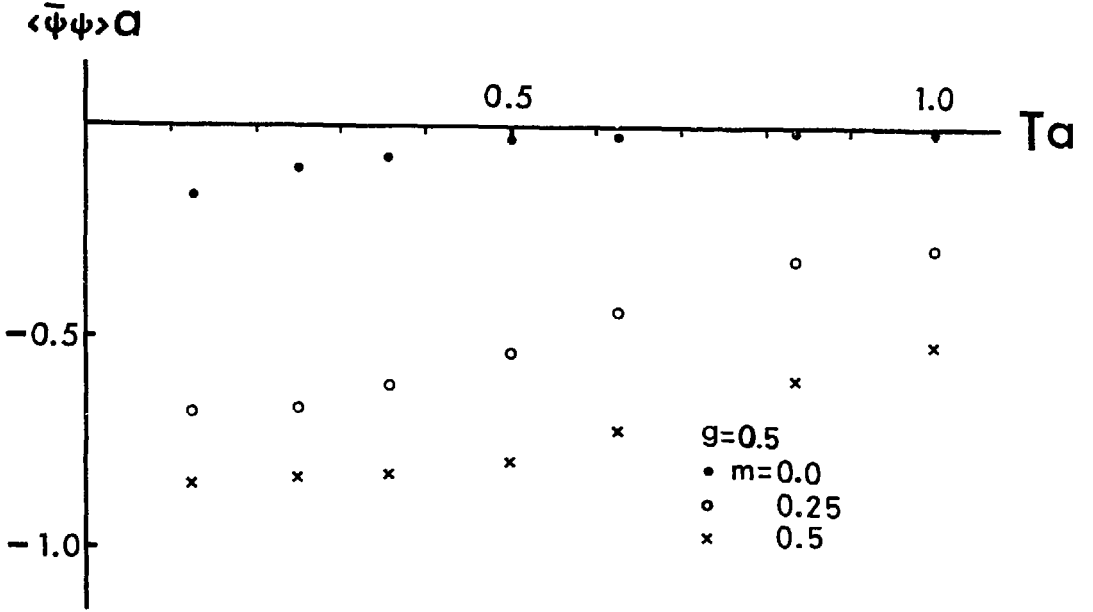

Fig. 6

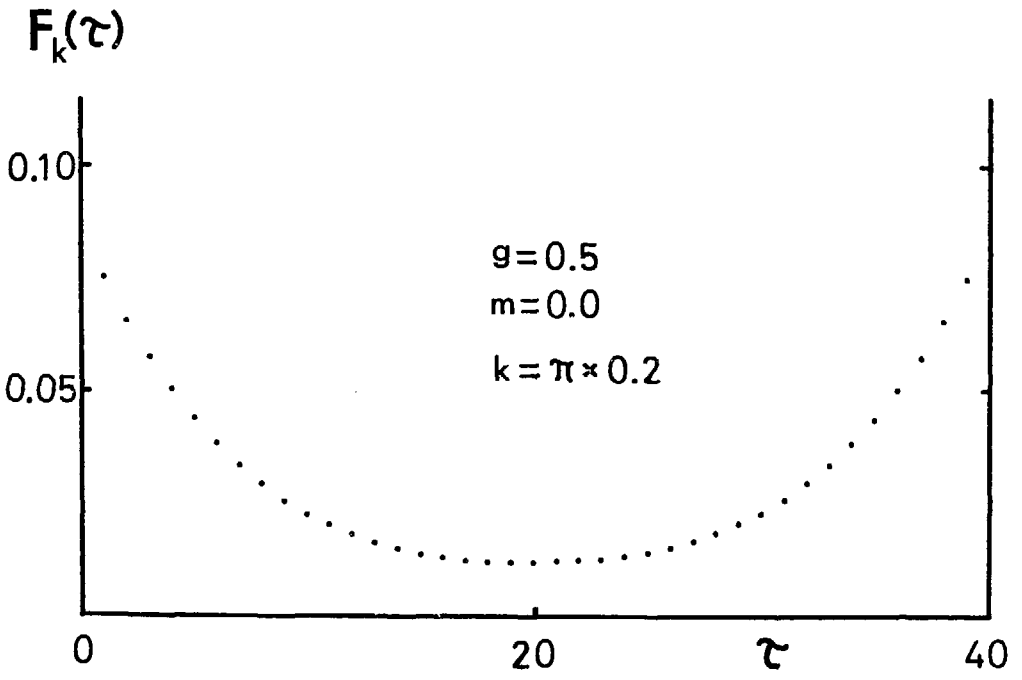

Fig. 7